On the utilization of radial extrusion to characterize fracture forming limits. Part II: testing and modelling

Sampaio, Rui F. V.; Pragana, João P. M.; Bragança, Ivo M.F. ; Silva, Carlos M.A. ; Nielsen, Chris V.; Martins, Paulo A.F.

Published in:
Sheet Metal 2023

Link to article, DOI:
10.21741/9781644902417-30

Publication date:
2023

Document Version
Publisher's PDF, also known as Version of record

Materials Research Proceedings **25** (2023) 237-244 https://doi.org/10.21741/9781644902417-30

On the utilization of radial extrusion to characterize fracture forming limits. Part II: testing and modelling

Rui F.V. Sampaio[1,a], João P.M. Pragana[1,b], Ivo M.F. Bragança[2,c], Carlos M.A. Silva[1,d], Chris V. Nielsen[3,e] and Paulo A.F. Martins[1,f *]

[1]IDMEC, Instituto Superior Técnico, Universidade de Lisboa, Portugal

[2]CIMOSM, Instituto Superior de Engenharia de Lisboa, Instituto Politécnico de Lisboa, Portugal

[3]Department of Civil and Mechanical Engineering, Technical University of Denmark

[a]rui.f.sampaio@tecnico.ulisboa.pt, [b]joao.pragana@tecnico.ulisboa.pt, [c]ibraganca@dem.isel.ipl.pt, [d]carlos.alves.silva@tecnico.ulisboa.pt, [e]cvni@dtu.dk, [f]pmartins.tecnico.ulisboa.pt

Keywords: Forming, Failure, Stress State Transitions

Abstract. This second part of the paper is focused on double-action radial extrusion testing and modelling to characterize material formability and failure in the bulk-to-sheet material flow transitions that are commonly found in metal forming. Results show that three-dimensional to plane-stress evolutions at the radially extruded flanges lead to different modes of fracture (by tension and by shear) that may or may not be preceded by necking. The use of double-action radial extrusion as a formability test also reveals adequate to characterize the failure limits of very ductile metallic materials, which cannot be easily determined by conventional upset compression tests, and to facilitate the identification of the instant of cracking and of the corresponding fracture strains by combination of the force vs. time evolutions with the in-plane strains obtained from digital image correlation.

Introduction

Competition between cracking opening modes by tension (mode I) and by out-of-plane shearing (mode III) in conventional bulk formability tests give rise to an 'uncertainty region' in principal strain space, as it was recently observed by Sampaio et al. [1]. Although research on formability and crack opening modes has been taking the competition between crack opening modes into account, there are aspects related to material flow transitions in regions of bulk metal forming parts subjected to extensive plastic material flow that are not commonly taken into consideration. Accountability of these aspects means, in practical terms, to include the three-dimensional to plane stress material flow transitions (i.e., bulk-to-sheet evolutions) in the list of parameters that are responsible for the competition between the different crack opening modes.

Under these circumstances, the main objective of this second part of the paper is to investigate formability in three-dimensional to plane stress material flow transitions by means of a new formability test based on the working principle of double-action radial extrusion [2]. It must, however, be said that the relevance of the new proposed formability test goes beyond the above-mentioned material flow transitions because it provides two significant advantages over the existing bulk formability tests.

Firstly, it allows carrying out tests with very slender cylindrical specimens, which would inevitably collapse by buckling during upset compression tests between flat parallel platens. This overcomes the difficulty of obtaining the experimental strains at fracture in very ductile materials, a topic that was also addressed by Bulzak et al. [3] when studying damage evolution in hot forming with rotary compression tests. However, the experimental evaluation of surface strains becomes very difficult for this test, due to the continuous movement of the specimen.

Materials Research Proceedings **25** (2023) 237-244 https://doi.org/10.21741/9781644902417-30

Secondly, the fact that triggering and subsequent propagation of cracks in the double-action radial extrusion test will always lead to force drops in the force vs. time evolutions. This allows determining the instant of cracking and of the corresponding fracture strains by combination of the experimental force vs. time evolutions with the results obtained from digital image correlation (DIC). In fact, the force vs. time evolution of the double-action radial extrusion test is different from those found in conventional upset compression tests in which the combination of surface expansion with strain hardening commonly prevents the force from dropping at the onset of cracking.

Experimental testing conditions

The double-action radial extrusion formability tests were carried out in a multidirectional tool set that was installed in a hydraulic testing machine. Fig. 1 shows a detail of the tool set in which the movement of the extrusion punches (P) towards each other inside the dies (D) is obtained by means of two cam slide units consisting of a punch holder (H) and a die wedge actuator (A) with a working angle $\alpha = 30°$. Two guided pillars (G) ensure the alignment between the upper and lower tool halves. Further details on the tool set and on the conversion of the vertical force F_v of the hydraulic testing machine into the horizontal force F_h applied by the extrusion punches are given in the first part of this paper (Part I).

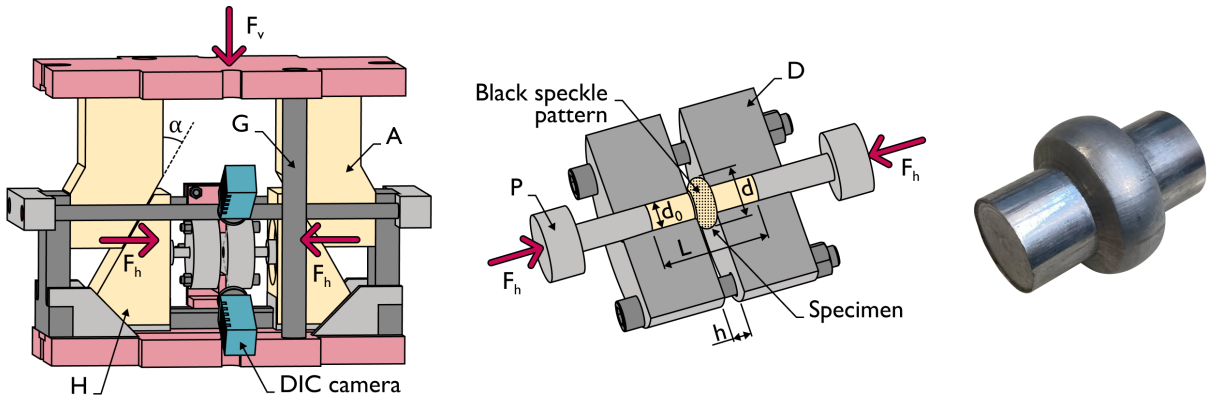

Fig. 1 Tool set for performing the double-action radial extrusion formability tests showing the cameras used by digital image correlation, the detail of the dies and punches and a test specimen.

The tests were carried out in a soft aluminum AA1050-O and a medium strength aluminum-magnesium-silicon alloy AA6082 in the annealed (O) and solution heat-treated (T6) state. The specimens were machined from the supplied rods and a molybdenum disulphide (MoS2) based lubricant was utilized in the operating testing conditions provided in Table 1.

Results and Discussion

Strain-Loading Paths in Principal Strain Space. Fig. 2 shows the experimental evolutions of the major and minor in-plane strains with time determined by DIC and of the radial extrusion force F_h with time after conversion of the vertical force F_v measured by the load cell. The in-plane strain evolutions were taken from the outer flange surface for the three different materials.

As seen, the instant of fracture t_f (refer to 'F' in Figs. 2a-c) is clearly recognized by a sudden drop in force and allows determining the major ε_1 and minor ε_2 in-plane strains at fracture from their evolutions with time $(\varepsilon_1, \varepsilon_2) = f(t)$ obtained from DIC. Point 'I' is the location in the outer flange surfaces where the strain evolutions were obtained.

Table 1 Operating conditions utilized in the double-action radial extrusion tests.

Dies	Gap height h	12 mm, 16mm, 32mm
	Fillet radius r	0.5 mm
Punches	Diameter	16 mm
	Velocity	5 mm/min
Specimens	Initial diameter d_0	16 mm
	Initial length l_0	50mm, 90mm
	Aspect ratio h/d_0	0.75, 1, 2

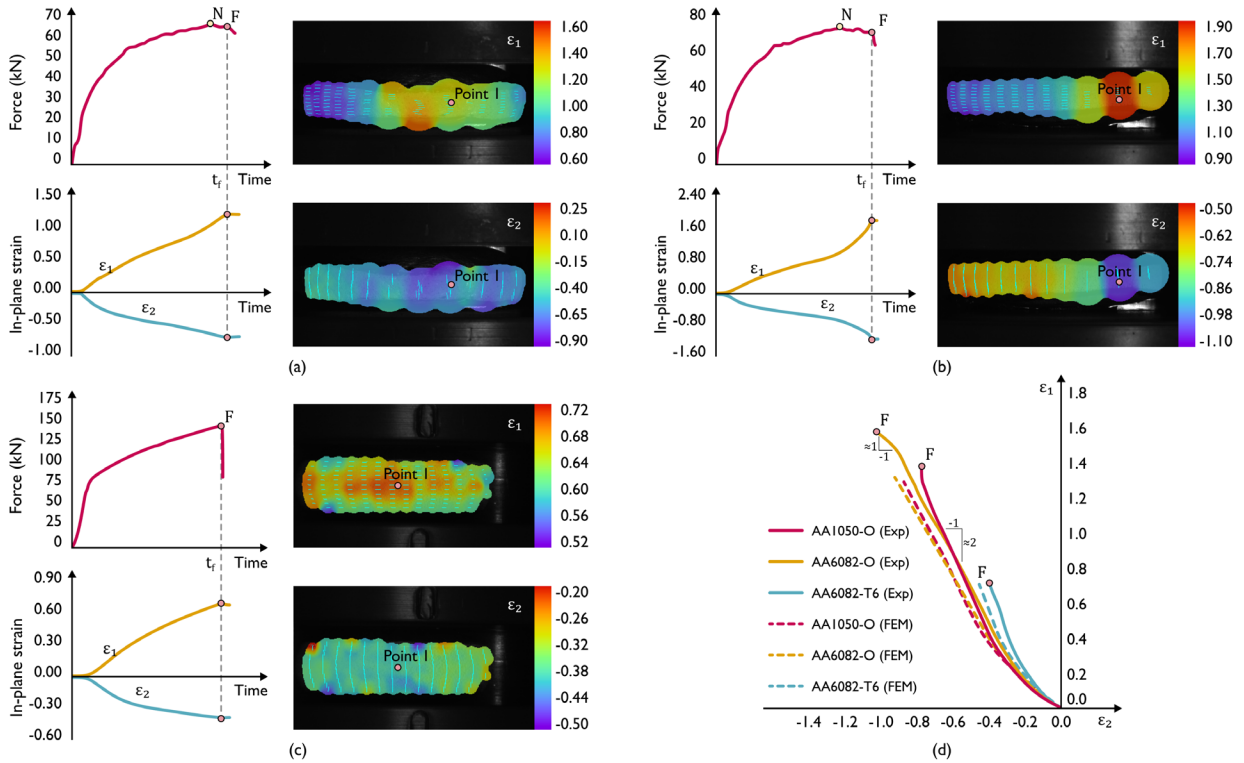

Fig. 2 Experimental evolutions of the force with time and of the major and minor in-plane strains with time for specimens with $h/d_0 = 0.75$ made from aluminum (a) AA1050-O, (b) AA6082-O and (c) AA6082-T6. The images were taken from DIC immediately before fracture. (d) Experimental and finite element predicted strain loading paths in principal strain space.

In case of the specimens made from aluminum AA1050 and AA6082 in the annealed (O) state, the instant of fracture is preceded by a change in the rate of force growth with time leading to the development of a neck on the outer flange surface (refer to 'N' in the force peaks of Figs. 2a, b). In contrast, the specimens made from aluminum AA6082-T6 only experience a sudden drop in force because cracking is not preceded by necking, as it was experimentally observed and will be shown later.

Application of the methodology that was described in the first part of this paper allows plotting the corresponding strain loading paths $\varepsilon_1 = f(\varepsilon_2)$ in principal strain space. The result is shown in Fig. 2d and allows distinguishing between monotonic and non-monotonic evolutions up to fracture thanks to the absence of necking (AA6082-T6) and to the sharp bends of the strain loading paths (in point 'F') towards plane strain (AA1050-O) and pure shear (AA6072-O) deformation conditions that happen in the specimens where fracture is preceded by necking.

Finite element computed evolutions of the strain loading paths (refer to the dashed lines in Fig. 2d) show a good agreement with DIC. However, the numerical estimates for the soft

aluminum AA1050 and the medium strength aluminum-magnesium-silicon alloy AA6082 in the annealed (O) state are only provided up to the onset of localized necking, which corresponds to approximately 80% of the total stroke. Beyond this point, the growth rate of the in-plane strains is very fast and the uncoupled finite element damage models utilized by the authors experience difficulties in handling the non-homogeneous plastic deformation and the elastic unloading caused by damage-induced softening.

However, because the onset of localized necking and point 'F' occur almost instantly, finite elements will continue to be used in the following sections of the paper to analyze the deformation mechanics and the different modes of failure that were observed in the double-action radial extrusion formability test.

Deformation Mechanics. Figs. 3a-c shows the initial and intermediate rotationally symmetric meshes at 30% of the total stroke for specimens with an aspect ratio $h/d_0 = 0.75$ made from the different materials and supplied conditions that were utilized in the investigation. As seen in the predicted distribution of vertical stresses, the radially extruded flanges start showing signs of three-dimensional to plane stress material flow transitions at the outer flange surfaces, which will become more pronounced as radial extrusion continues and the flange diameter increases.

The aspect ratio h/d_0 of the specimens plays a key role in the utilization of radial extrusion as a formability test capable of monitoring the three-dimensional to plane stress material flow transitions. In fact, larger aspect ratios than those shown in Figs. 3a-c, do not give rise to plane stress conditions (Fig. 3d) and may result in material flaws (Fig. 3e) or buckling, as reported in earlier investigations of the radial extrusion process [4]. In such situations not only the diameter-to-thickness ratio of the radially extruded flanges deviates from typical sheet forming values as plane stress conditions no longer prevail on the outer flange surfaces.

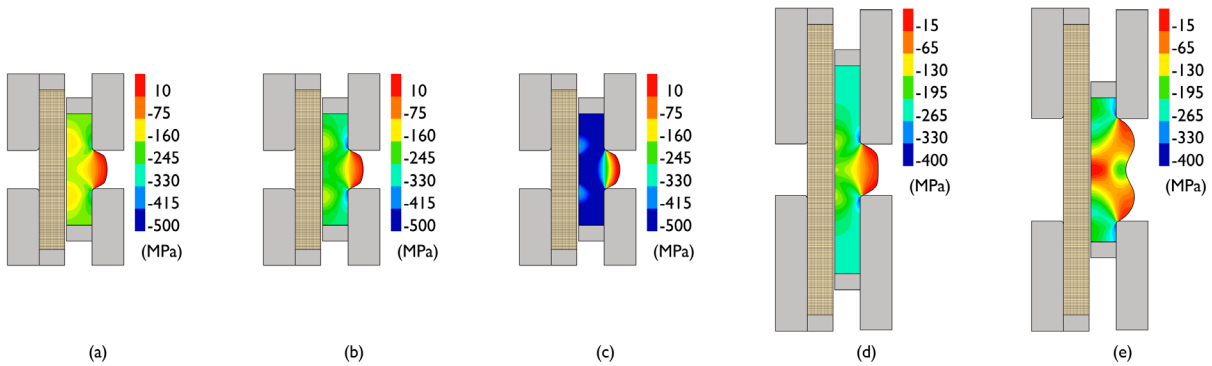

Fig. 3 Initial and intermediate rotationally symmetric meshes with finite element predicted distribution of vertical stress for specimens made from aluminum: (a) AA1050-O with $h/d_0 = 0.75$, (b) AA6082-O with $h/d_0 = 0.75$, (c) AA6082-T6 with $h/d_0 = 0.75$, (d) AA1050-O with $h/d_0 = 1$ and (e) AA1050-O with $h/d_0 = 2$.

The asymmetric deformation of the three specimens with an aspect ratio $h/d_0 = 0.75$ that progressively develops during the final stage of the double-action radial extrusion test was simulated with the three-dimensional finite element model built upon the interaction between two and three-dimensional meshes that was earlier described. For this purpose, the authors artificially imposed small gauge imperfections of approximately 0.2 mm on the outer flange diameter located at the vicinity of the xz-plane. These imperfections account for less than 1% of the flange diameter and correspond to localized material weaknesses that resemble those utilized by Marciniak and Kuczynski [5] in their theory of plastic instability in sheet metal forming.

The result of the above-mentioned strategy combined with intermediate remeshing operations aimed at replacing elements with excessive distortion at the center of the specimens made from

AA1050-O and AA6082-O is disclosed in Fig. 4. As seen, finite element computed geometries obtained shortly after the onset of cracking agree well with the experimental test specimens.

Incipient crack propagation was numerically modelled by means of an element deletion (removal) technique based on the critical value of a damage function D,

$$D = \int_0^{\bar{\varepsilon}} g \, d\bar{\varepsilon} \tag{1}$$

where g is a weight function and $\bar{\varepsilon}$ is the effective strain. Two different weight functions were used: (i) the McClintock [6] stress triaxiality ratio $g_{Mc} = \sigma_m/\bar{\sigma}$, corresponding to failure by tension (mode I), where σ_m is the hydrostatic stress and $\bar{\sigma}$ is the effective stress (Fig. 4a) and (ii) the Cockcroft-Latham [7] normalized principal stress ratio $g_{CL} = \sigma_1/\bar{\sigma}$, corresponding to failure by out-of-plane shear (mode III), where σ_1 is the major principal stress (Figs. 4b, c).

The choice between the proper weight function g to be used for each test case was based on the strain loading path evolutions disclosed in Fig. 2d, which clearly indicate failure by tension preceded by necking in AA1050-O, by out-of-plane shear preceded by necking in AA6082-O and failure without previous necking in AA6082-T6.

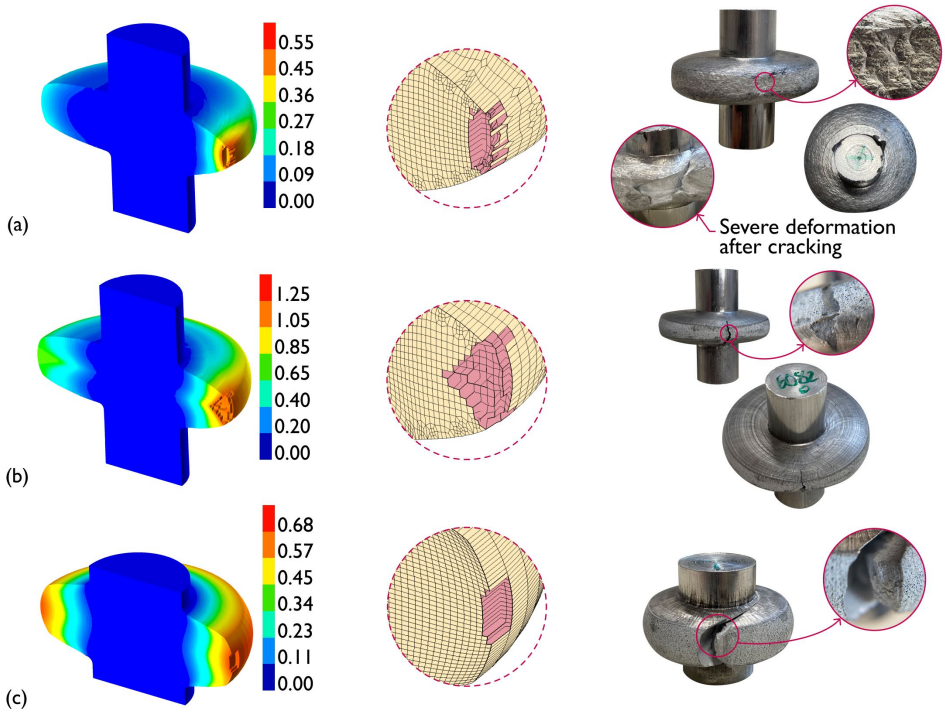

Fig. 4 Three-dimensional finite element prediction of ductile damage with mesh details showing cracks on the outer flange surfaces for three different test specimens with an aspect ratio $h/d_0 =$ 0.75 *made from aluminum (a) AA1050-O, (b) AA6082-O and (c) AA6082-T6. Ductile damage was calculated according to (a) McClintock [6] and (b, c) Cockcroft-Latham [7] criteria and photographs of the specimens are enclosed for comparison purposes.*

Further observation of the two different types of necks combined with fractography analysis by means of scanning electron microscopy (SEM) to be presented in the next section provides a better identification and understanding of the different types of failure and modes of deformation that are likely to occur in three-dimensional to plane stress material flow transitions.

Necking and Fractography. Combination of the finite element computed meshes with the images obtained from DIC and SEM (Fig. 5) allows concluding that fracture in the outer surface flange of the AA1050-O test specimens is by tension (mode I). Results also show evidence of

Materials Research Proceedings **25** (2023) 237-244 https://doi.org/10.21741/9781644902417-30

plastic instability in the form of diffuse (Fig. 5a) and localized necking (Fig. 5c) in good agreement with the deformation mechanics of sheet forming. In fact, the localization of the neck along a direction inclined at an angle of approximately 53.2° (Fig. 5c) to the circumferential direction value is very close to the theoretical estimate of 54.7° (Fig. 5b) obtained for a sheet (plane stress) specimen made from an isotropic material, subjected to uniaxial tension [8].

The morphology of the cracks consists of circular dimple-based structures (Fig. 5d), and further corroborates the experimental observation of cracks opening by tension (mode I) and running radially along the flange.

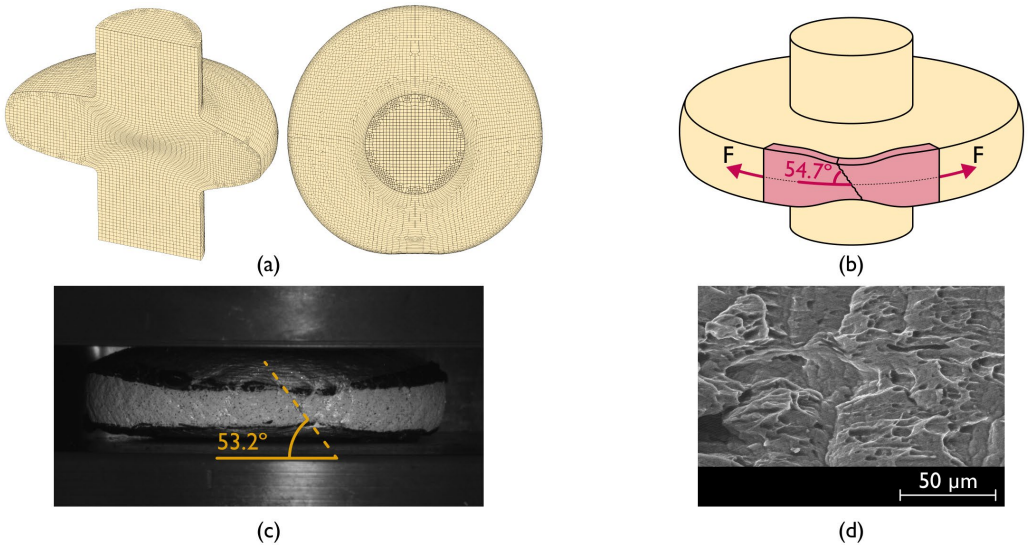

Fig. 5 Failure mode of the aluminum AA1050-O test specimen with an aspect ratio $h/d_0 = 0.75$ *showing (a) the computed finite element mesh, (b) the analogy with localized necking in uniaxial tension of a sheet test specimen, (c) a DIC image showing localized necking at the outer flange surface and (d) a SEM picture showing the morphology of the cracks.*

Application of the same methodology for the specimens made from AA6082-O (Fig. 6a) confirms that vertical cracks opened by shear stresses due to the occurrence of smooth parabolic dimple-based structures (Fig. 6e). Moreover, these cracks do not run radially along the flange (Fig. 4b), as it is commonly observed in the upset compression of cylindrical and tapered test specimens, due to significant distortion of outer flange surface placed within the neighborhood of the localized neck. All this is consistent with the strain path bend towards pure shear in principal strain space (Fig. 2d) before failing by through-thickness shearing (mode III).

The pure shear stress state acting at the outer flange surface (with $\varepsilon_\theta = -\varepsilon_z > 0$) gives rise to plane strain deformation along the radial direction ($\varepsilon_r = 0$) due to material incompressibility. Thus, assuming these conditions to hold in-between the top and bottom flange surfaces due to combination of small thickness and plane stress material flow conditions, an analogy with uniaxial tension of a sheet test specimen can also be made.

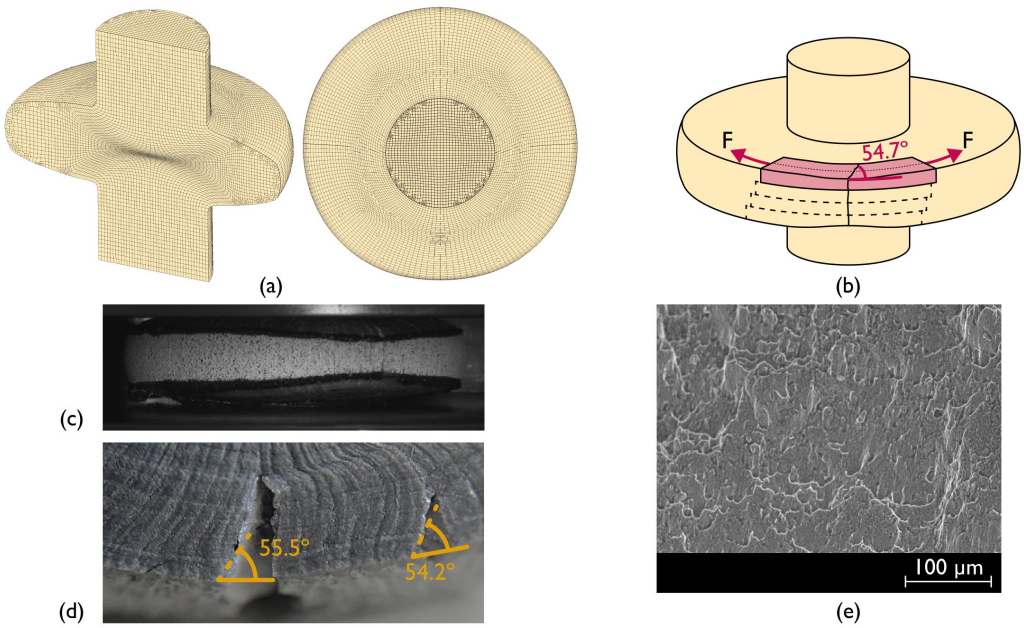

Fig. 6 Failure mode of the aluminum AA6082-O test specimen with an aspect ratio $h/d_0 = 0.75$ *showing (a) the computed finite element mesh, (b) the analogy with pure shear within the neighborhood of the localized neck, (c) a DIC image showing localized necking along the longitudinal direction at the outer flange surface, (d) top view detail of the flange near the neck showing crack opening on the* r-θ *plane with angles and (e) a SEM picture showing the morphology of the cracks.*

The analogy requires a similar approach to that taken for the specimen made from AA1050-O but now with diffuse necking taking place in the radial direction (Figs. 6b and 6c) and crack opening in the r-θ plane after the occurrence of localized necking with angles of approximately 54° ~ 55° (refer to the top flange view in Fig. 6d).

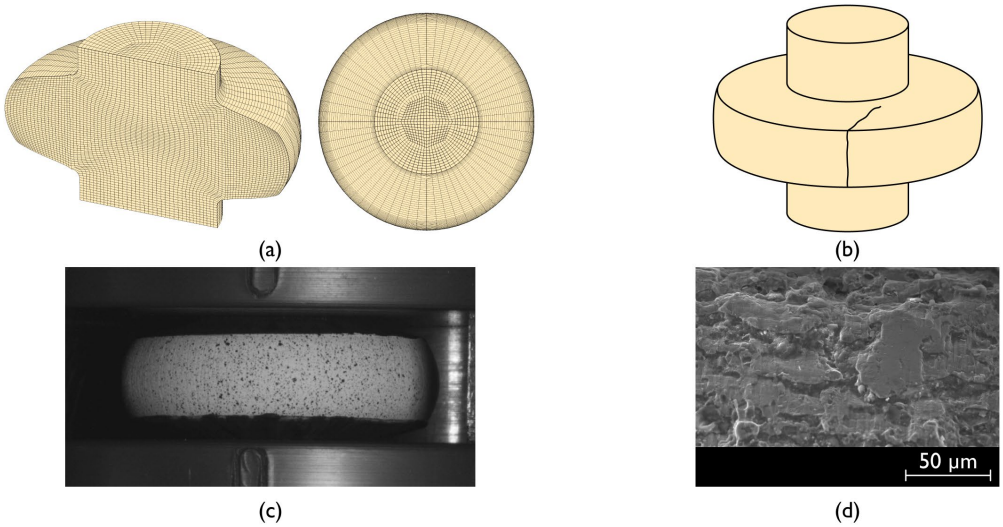

Fig. 7 Failure mode of the aluminum AA6082-T6 test specimen with an aspect ratio $h/d_0 = 0.75$ *showing (a) the computed finite element mesh, (b) a scheme showing vertical cracks that do not propagate radially, (c) a DIC image showing the absence of necking at the onset of cracking and (d) a SEM picture showing the morphology of the cracks.*

In what concerns the results obtained for the specimens made from AA6082-T6 (Fig. 7a) it is possible to conclude that vertical cracks open without previous necking (Fig. 7c). Crack

propagation does not run radially, as it is schematically disclosed in Fig. 7b, due to the development of a mixed mode characterized by the simultaneous occurrence of circle and smooth parabolic dimple-based structures (Fig. 7d).

Conclusions

The work on the utilization of double-action radial extrusion as a new formability test to characterize failure in bulk-to-sheet material evolutions led to the following main conclusions:

- The test can be successfully used to characterize material formability in the three-dimensional to plane stress material flow transitions that are commonly found in bulk metal formed parts,
- Material flow transitions give rise to uniaxial tension states of stress that eventually lead to crack opening with or without previous localized necking,
- Cracks preceded by localized necking develop under plane strain or pure shear material flow conditions on the outer flange surface,
- The morphology of the cracks reveals crack opening by tension (mode I), by shear (mode III) and by a mixed mode resulting from combination of modes I and III,
- The new test is also adequate to characterize the formability limits of very ductile materials with large fracture strains, such as aluminum AA1050-O and AA6082-O, which cannot be easily determined by conventional upset compression tests.

Acknowledgements

The authors would like to acknowledge the support provided by Fundação para a Ciência e a Tecnologia of Portugal and IDMEC under LAETA- UIDB/50022/2020 and PTDC/EME-EME/0949/2020.

References

[1] R.F.V. Sampaio, J.P.M. Pragana, I.M.F. Bragança, C.M.A. Silva, P.A.F. Martins, Revisiting the fracture forming limits of bulk forming under biaxial tension, International Journal of Damage Mechanics 31 (2022) 882-900. https://doi.org/10.1177/10567895211072580

[2] R. Balendra, Process mechanics of injection upsetting, International Journal of Machine Tool Design and Research 25 (1985) 63-73. https://doi.org/10.1016/0020-7357(85)90058-7

[3] T. Bulzak, Z. Pater, J. Tomczak, Ł. Wójcik, A rotary compression test for determining the critical value of the Cockcroft–Latham criterion for R260 steel, International Journal of Damage Mechanics 29 (2020) 874–886. https://doi.org/10.1177/1056789519887527

[4] R. Balendra, Y. Qin, Injection forging: engineering and research, Journal of Materials Processing Technology 145 (2004) 189-206. https://doi.org/10.1016/S0924-0136(03)00670-8

[5] Z. Marciniak, K. Kuckzynski, Limit strains in the process of stretch-forming sheet metal, International Journal of Mechanical Sciences 9 (1967) 609–620. https://doi.org/10.1016/0020-7403(67)90066-5

[6] F.A. McClintock, A Criterion for ductile fracture by the growth of holes, Journal of Applied Mechanics 35 (1968) 363–371. https://doi.org/10.1115/1.3601204

[7] M.G. Cockroft, D.J. Latham, Ductility and the workability of metals, Journal of the Institute of Metals 96 (1968) 33–9.

[8] R. Hill, A theory of yielding and plastic flow of anisotropic metals, Proceedings of the Royal Society, London, Series A 193 (1948) 281–297. https://doi.org/10.1098/rspa.1948.0045